Single Centrosome Manipulation Reveals Its Electric Charge and Associated Dynamic Structure

S. Hormeño,[†] B. Ibarra,[†] F. J. Chichón,[†] K. Habermann,[‡] B. M. H. Lange,[‡] J. M. Valpuesta,[†] J. L. Carrascosa,[†] and J. R. Arias-Gonzalez[†§*]

[†]Department of Macromolecular Structure, Centro Nacional de Biotecnología, CSIC, Madrid, Spain; [‡]Department of Vertebrate Genomics, Max Planck Institute for Molecular Genetics, Berlin, Germany; and [§]Instituto Madrileño de Estudios Avanzados en Nanociencia, Madrid, Spain

ABSTRACT The centrosome is the major microtubule-organizing center in animal cells and consists of a pair of centrioles surrounded by a pericentriolar material. We demonstrate laser manipulation of individual early *Drosophila* embryo centrosomes in between two microelectrodes to reveal that it is a net negatively charged organelle with a very low isoelectric region (3.1 $\pm$ 0.1). From this single-organelle electrophoresis, we infer an effective charge smaller than or on the order of 10^3 electrons, which corresponds to a surface-charge density significantly smaller than that of microtubules. We show, however, that the charge of the centrosome has a remarkable influence over its own structure. Specifically, we investigate the hydrodynamic behavior of the centrosome by measuring its size by both Stokes law and thermal-fluctuation spectral analysis of force. We find, on the one hand, that the hydrodynamic size of the centrosome is 60% larger than its electron microscopy diameter, and on the other hand, that this physiological expansion is produced by the electric field that drains to the centrosome, a self-effect that modulates its structural behavior via environmental pH. This methodology further proves useful for studying the action of different environmental conditions, such as the presence of Ca^{2+}, over the thermally induced dynamic structure of the centrosome.

INTRODUCTION

The centrosome is a complex organelle in higher eukaryotic cells that usually lies near the center of the cell and in close proximity to the nucleus (1,2). Its structure is highly heterogeneous in different cell types and organisms (3), but normally it is composed of a pair of centrioles surrounded by the so-called pericentriolar material (PCM). Centrioles are barrel-shaped structures that lie perpendicular to one another and in close proximity at one end (4–6). Generally, they comprise nine triplets of microtubules, together with other elements. The PCM is a fibril matrix that provides the centrosome with a scaffold for anchoring proteins that are involved in microtubule nucleation and other activities. It acts as a highly dynamic molecular lattice that contributes to both the morphology and activity changes of the centrosome during the cell cycle (1,2,7,8). Development of the centrosome is much more complex than that of other organelles and involves duplication during the cell cycle. This unique ability, which is shared only by chromosomes, seems to be linked to the cell progression cycle in, for example, the activation of the final stages of cytokinesis and in the release of cells from a checkpoint. It also needs to be coordinated with the chromosome cycle. The centrosome plays a relevant role in microtubule nucleation, anchoring, and release. These processes are essential for mitotic spindle assembly and positioning during cell division, and for cytoskeleton organization. They are also important for adhesion and regulating cell motility, and they influence cell polarity. Despite the importance of the centrosome, its precise molecular composition, structural features, function, and regulation have yet to be determined (1,2).

Electric phenomena, which are key to explaining molecular structure and interactions, demonstrate subtle but essential roles in cellular processes on the nanoscale (9). Local electric fields and charged structures are ubiquitous in the cell (10,11), and hence the electrical nature of a large supramolecular assembly is of critical concern. The highly dense cellular medium nurtures a complex dynamics that involves a multitude of local, albeit globally integrated, processes. In this scenario, large charged structures, such as microtubules, membranes, or the cytoskeleton (12–16), should be involved in the marshalling and motion of macromolecules (9–11). Small, direct electric fields can influence important processes such as cell division (17), and in this context the electrical properties of the centrosome are fundamental to understanding its interactions, diffusion, and function inside the cell. In addition, because of the large dimensions of a centrosome and the absence of a definite boundary, size, and shape, an electrical charge has self-structural implications.

Here we report a basic physical property—the electrical charge (q)—of a fundamental biological element, the centrosome. Our experiments demonstrate both the significance of nanoscale electrostatics in the cell and the roles played by this organelle (previous studies provided only hypotheses regarding this subject (14,15)). We concurrently characterize the centrosome hydrodynamic behavior in physiological conditions, and find that it is linked to its electric behavior. The diffusive nature of the PCM further makes this hydrodynamic description necessary to understand the interplay between the structural dynamics of the centrosome and the thermal fluctuations of the aqueous bath. We measure

Submitted March 25, 2009, and accepted for publication June 1, 2009.

*Correspondence: ricardo.arias@imdea.org

Editor: Alberto Diaspro.

0006-3495/09/08/1022/9 $2.00

doi: 10.1016/j.bpj.2009.06.004

a surface-charge density for the centrosome that is smaller than that of microtubules (its immediate functional partners) by 1–2 orders of magnitude (12,13). We find, however, a major effect on its own structure. Specifically, we show, from the study of its hydrodynamic behavior, that the electric field that ensues from this organelle self-induces a pH-dependent structural dynamics that modulates the PCM structure.

A large supramolecular assembly is a complex system whose charge and isoelectric point (pI) are difficult to infer from a direct examination of its molecular parts, because its higher level of organization plays a role in charge distribution. The pI of microtubules is ~4.2 (12), which is significantly lower than that of individual tubulin monomers (5.45–5.65 and 5.30–5.45 for α and β tubulin, respectively (18,19)). The unknown molecular and structural details of the centrosome make this macromolecular assembly even more elusive for predictions. Therefore, to investigate these phenomena, we devised a way to perform laser manipulation (20) of single centrosomes. Ashkin and Dziedzic (21,22) paved the way for the optical trapping and manipulation of individual biological specimens, such as viruses, cells, and even organelles located within living cells, without optical damage. A further development by Fuhr and co-workers (23) combined high-frequency electric fields with optical manipulation of both single particles and single cells in an electro-optical trap. Our single-organelle methodology, which complements bulk assays, is also valuable for investigating a centrosome's sensitivity to different conditions or buffering constituents, such as Ca^{2+}.

The charge of the centrosome is an important factor in both the structural and physicochemical dynamics of a cell; furthermore, its resultant electric near field may also play a role in recruiting tubulin dimers at distances on the order of the Debye length by orienting their electric dipoles in the organelle's vicinity. This passive mechanism for nascent microtubules may help the action of microtubule plus-end binding proteins over diffusing tubulin dimers (24,25) in the early growing of microtubules near the centrosome. In addition, given the fact that both the centrosome and the lateral surface of microtubules present the same polarity, electric forces among this organelle and the microtubule walls give rise to a radial direction of growth to the emerging microtubules off the centrosome. Both phenomena may assist in an organized, early development of the aster, and thus may have a functional role in centrosome-mediated cellular processes, such as mitosis.

MATERIALS AND METHODS

Centrosome preparation

Centrosomes were prepared from early *Drosophila* embryos, as detailed elsewhere (5,26). Sucrose fractions were assayed for centrosomes by immunofluorescence microscopy with the anti-γ-tubulin antibody GTU-88. Peak fractions were aliquoted, frozen in liquid nitrogen, and stored at -80°C. A few centrosomes obtained from the preparation were imaged by low-resolution cryo-electron microscopy (cryo-EM) to check the quality of the purification (see the Supporting Material). Room temperature was (24 ± 2)$^{\circ}$C throughout the experiments.

Experiments with optical tweezers

The optical design includes a dual-counterpropagating-beam ($\lambda = 835$ nm) optical trap capable of measuring forces as changes in light momentum flux (27). We used the double-beam trap geometry for control experiments with polystyrene beads and for the size determination experiments with single centrosomes. However, we used a single-beam trap for the electric measurements of single centrosomes to increase the force sensitivity of the optical transducer in the subpicoNewton range. The force measured by a light-momentum sensor calibrated from first principles (conservation of linear momentum) does not depend on either the power or the direction of the incident radiation provided that all the scattered light is collected and there is no absorption (27). The power on the biological specimen was kept constant at ~70 mW or 140 mW (single-beam geometry or dual-counterpropagating-beam geometry, respectively). The two objectives used in this optical-tweezers design are Nikon CFI Plan-Apochromat 60× (Nikon, Tokyo, Japan), water immersion, numerical aperture (NA) 1.2. Each objective is used to both focus and collect light for analysis. The NA of each single beam is ~0.5. We used low-NA beams inside high-NA objectives to allow for significant beam deflection while still collecting all the light, thus ensuring force measurement by the calibration based on the conservation of light momentum (27). This has the additional advantage of reducing both the energy concentration (once the incident power is set, the volume of the focal region increases when the beam NA decreases, with a subsequent decrease of the power per unit volume in the trapping region) and the gradient forces, which diminishes optical damage and internal stress on the biological specimen. Centrosomes and control beads were trapped and manipulated with the optical tweezers inside a fluid chamber. More specifically, they were flowed into the chamber by means of a fluidics system that consisted of glass microdispensers and polyethylene tubes connected to the sample reservoirs, as described elsewhere (20). With this method, buffers can be easily exchanged and centrosomes can be flowed at a controlled rate, enabling the detection of impurities and avoiding aggregates.

Electric force measurements

The fluid chamber was designed to accommodate two 25-μm-thick gold-plated tungsten wires (Luma-Metall, Kalmar, Sweden) separated by 1–2 mm. In brief, the fluid chamber was built by using two microscope coverglasses sandwiching two parafilm layers with imprinted channels. The distance between the inner faces of the chamber was ≈ 200 μm. The electrode wires were inserted in the central channel and stuck between the two parafilm layers through glass tubes to control both separation and parallelism between the wires. The optical trapping position of the beads or centrosomes was kept equidistant with respect to the two wire electrodes. Constant-voltage pulses were applied in the range of 3–5 V. Voltage strength and pulse frequency were chosen to prevent buffer electrolysis and subsequent fluid flows due to bubbles.

Buffers and beads

The physiological size of the centrosome was determined in BRB80 buffer (80 mM K-PIPES, 1 mM $MgCl_2$, 1 mM EGTA, pH 6.8). To test the effect of calcium, we used 80 mM K-PIPES, 1 mM $MgCl_2$, 5 mM $CaCl_2$, pH 6.8. The electric properties of the centrosome and the associated sizes at different pH values were measured in a variety of buffers with diluted concentrations of the stock solutions. This condition was desired to both decrease the ionic strength of the solutions and hence avoid strong electric shielding that could hinder the observable electric response, and to decrease the conductivity of the solutions and hence avoid the formation of bubbles due to electrolysis. For electric measurements, we used TAE buffer (40 mM Tris-acetate, 2 mM EDTA) for pH 8.19, with conductivity $\sigma = 2.360$ mS/cm and ionic strength 96 mM. Acetate buffers at pH 2.92, 3.10, 3.13, and 3.64, with

$\sigma = 0.450$, 0.413, 0.399, and 0.655 mS/cm and ionic strengths of 96.43, 100, 100, and 100 mM, respectively, were prepared by titrating sodium acetate with acetic acid. Finally, pH 2.66 with $\sigma = 2.050$ mS/cm and ionic strength 12.12 mM was obtained by titrating potassium chloride with chloride acid. When deionized (DI) water (Milli-Q water purification system (Millipore, Billerica, MA), conductivity 5.5×10^{-5} mS/cm at 25°C) was used at pH 7.60, conductivity was increased by either the addition of phosphate-buffered saline (PBS) in experiments with beads, or BRB80 buffer in experiments with centrosomes, up to final values of 0.0822 and 0.0535 mS/cm and ionic strengths of 0.0765 and 1.7 mM. For reference to the size experiments, we used a variety of microspheres, i.e., 0.53- and 3.18-μm-diameter polystyrene beads and streptavidin-coated, 2.10-μm-diameter polystyrene beads purchased from Spherotech (Libertyville, IL). For reference to measurements of the centrosome's electric properties, we used streptavidin-coated, 2.10-μm beads. We characterized their electric behavior by measuring their electrophoretic mobility in each buffer used (see the Supporting Material), and we confirmed agreement with the previously reported pI of surface monolayers of streptavidin (28).

Hydrodynamic size analysis

Stokes law size determination

The force required to drag a small (low Reynolds number) object immersed in a fluid is $F = \gamma v$ (Stokes law), where γ is the drag coefficient of the object and v is its velocity relative to the fluid. We assumed on average a spherical morphology for the early *Drosophila* embryo centrosome (see the Results for details); then, $\gamma = 3\pi d\eta$, where d is the hydrodynamic or Stokes diameter of the object and η is the viscosity of the medium. To obtain d, different flow velocities were generated by manually moving the fluidics chamber back and forth in the x axis using a translation stage (Thorlabs MDT-631; Thorlabs, Newton, NJ) while the object was held in the optical trap and resulting drag forces were registered in the x direction. The velocity of the chamber was recorded using an LVDT sensor (Schaevitz PCA 116-100; Schaevitz Sensors, Hampton, VA). Assuming that the viscosity of the buffer is that of water at 25°C, i.e., $\eta_{water} = 0.894 \times 10^{-3}$ Pa · s, d can be recovered from the linear regression of the force-velocity data by using the aforementioned law.

Thermal-noise size determination

The equilibrium power spectral density of force fluctuations of an overdamped particle in a harmonic potential can be given by (29–31): $\langle \Delta F^2(f) \rangle_{eq} = 2\gamma k_B T f_c^2/(f^2 + f_c^2)$ in units of force squared per frequency, where $\langle \ldots \rangle$ represents the ensemble average, $f_c = \kappa/2\pi\gamma$ is the so-called corner frequency, γ is the drag coefficient of the particle, k_B is the Boltzmann constant, T is the temperature, κ is the spring constant of the particle in the optical trap, and f is the sampling frequency in units of hertz. The diameter, d, of the centrosome was derived from the drag coefficient by assuming on average a spherical shape, as explained above for the Stokes law method. To that end, a voltage signal proportional to the force exerted by the thermal fluctuations on a trapped centrosome was recorded in intervals of 5.24 s at 100 kHz. The time interval was then split into 128 parts of 40.96 ms. Next, force fluctuations (in voltage units) in each interval were Fourier transformed in the time domain $(-\infty, +\infty)$ and averaged over the 128 samples. Resulting data, in units of voltage squared per frequency, were fitted to the power spectral density equation shown above to obtain the drag coefficient of the centrosome, γ_{cs}. The same procedure was used to obtain the drag coefficient of polystyrene microspheres of known diameter, γ_{bead}, which, as mentioned above, we used for reference experiments. To set d in common units, we calibrated the size of the centrosomes, d_{cs}, thus measured, relative to that of the reference beads, d_{bead}, from the ratio of drag coefficients: $d_{cs} = d_{bead} \times \gamma_{cs}/\gamma_{bead}$.

RESULTS

Centrosomes prepared from early *Drosophila* embryos (5,7,26) were flowed at a controlled rate into a fluid chamber. Individual specimens were then trapped in different buffer solutions by means of a dual-beam optical tweezers system (27). This apparatus gives a direct measurement of the force exerted on a trapped specimen by the change in momentum flux in the trapping light beams due to their interaction with the trapped specimen. Since this method is not based on trap stiffness, force calibration is independent of the particle's size, shape, or refractive index; the viscosity or refractive index of the buffer; and variations in laser power (27). Centrosomes, whose size compares with optical wavelengths, become discernible in buffer solution by videomicroscopy due to their Brownian motion (see the Supporting Material and Movie S1 and Movie S2). Subsequent size analysis makes it possible to distinguish between single- and multiple-centrosome trapping events so that the latter can be discarded from the experimental data sets. In our experiments, an individual centrosome remained steadily trapped with both single- and dual-counterpropagating-beam traps with low NA (27) (see Materials and Methods) when external forces did not exceed ~10 pN and ~20 pN, respectively. This fact proves the centrosome as a biological specimen with a considerable dielectric constant at optical frequencies. This is consistent with having a large tubulin concentration (4) since this dimeric complex has a high dielectric constant (32).

Hydrodynamic behavior: the physiological size of the centrosome is 60% larger than its EM diameter

By optically maneuvering an individual centrosome in different buffer conditions, we were able to investigate its hydrodynamic behavior. Such a characterization, which to our knowledge has not been reported to date, is significant because the centrosome lacks a membrane that delimits its extent. We inferred the size of each specimen in physiological conditions (that is, in BRB80 buffer conditions, with both physiological pH 6.8 and 1 mM $MgCl_2$, which make the centrosomes functional in vitro) from measurements of its drag coefficient by means of two independent methods, namely, Stokes law and the thermal-fluctuation spectral analysis of force (see Materials and Methods). As a control, we performed these experiments with a variety of polystyrene microparticles of known diameter (see the Supporting Material). Fig. 1, *A* and *B*, illustrate the use of Stokes law and the analysis of thermal fluctuations of the optically held centrosome, respectively, and display the range of distances over which the centrosome is displaced in each method. The centrosome from an early *Drosophila* embryo has an overall spherical shape due to its abundant PCM (26), and consequently it constitutes a good model for the hydrodynamic characterization of this organelle. The action of thermal fluctuations over the diffusive PCM in aqueous solution averages out the molecular details at this dynamic level of resolution. The physiological size thus obtained for each centrosome is orientation-independent and hence it can be compared with

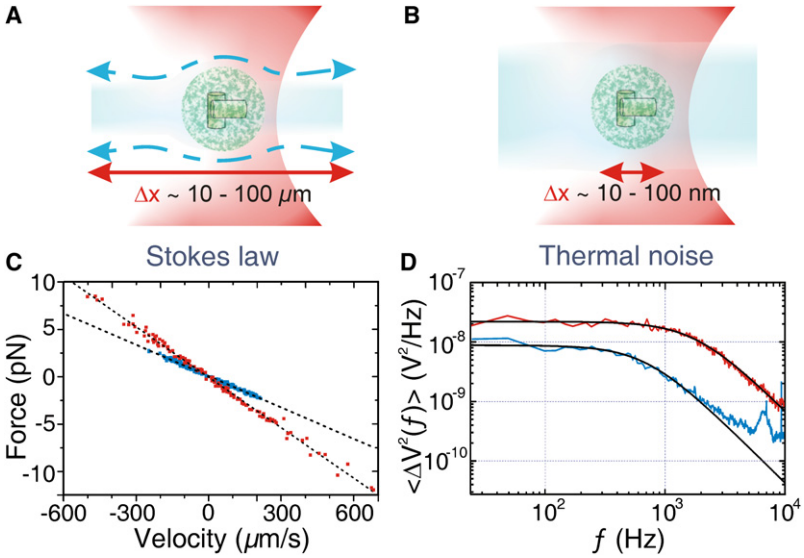

FIGURE 1 Hydrodynamic drag analysis of individual *Drosophila* centrosomes in physiological conditions. Two approaches were used: (*A*) Stokes law and (*B*) thermal-noise analysis. The plots further depict centrosome-neighborhood hydrodynamic size effects due the range of displacements used in each method (see the text for details). (*C*) Force versus velocity data for a centrosome in BRB80 buffer (*blue dots*) and a 2.10-μm-diameter polystyrene bead in DI water (*red dots*). Black dotted lines: Linear regressions. Inferred diameters for the centrosome and the 2.10-μm bead in this plot are 1.31 $\pm$ 0.01 and 2.10 $\pm$ 0.01 μm, respectively. (*D*) Power spectral density distribution of force fluctuations for a centrosome in BRB80 buffer (*blue line*) and a 2.10-μm-diameter polystyrene bead in DI water (*red line*). The units are volts squared per hertz (V^2/Hz) since we measure a voltage proportional to the fluctuating force. Only fluctuations in the horizontal direction were measured. Black curves: Fittings to the power spectral density function described in the Materials and Methods section. At both low and high frequencies, electronic noise may add to the thermal fluctuations, causing deviations from the expected spectrum. The corner frequencies for the centrosome and the 2.10-μm bead in this plot are 693 $\pm$ 13 Hz and 1795 $\pm$ 16 Hz, respectively, and the corresponding diameters are 0.87 $\pm$ 0.01 and 2.14 $\pm$ 0.01 μm. These measurements were taken by the dual-beam laser tweezers, with each diode-laser running at 200 mW and wavelength 835 nm.

previous EM characterizations that were performed, in contrast, in dehydration conditions (26).

Fig. 1, *C* and *D*, compare force versus velocity data and power spectral densities, respectively, of an individual centrosome and those of a 2.10-μm-diameter polystyrene bead trapped inside the fluid chamber at room temperature. Since the specimens were trapped >80 μm away from the surfaces of the fluid microchamber (i.e., a distance ~20 times the 2.1-μm-diameter bead), wall effects were negligible. For the Stokes law method (Fig. 1 *C*), we used low drag velocities for the centrosome to prevent deviations from linearity in the force-versus-velocity plot that could arise from bulk deformations of this organelle. As mentioned above, we kept a low beam NA (~0.5) in our optical-tweezers apparatus to exert weak transversal gradient forces over the biological specimen. This design further facilitates both translational and rotational diffusion of the centrosome, thus enabling the aforementioned self-averaging process in the measured size. In the thermal analysis method (Fig. 1 *D*), the spectrum curves that correspond to the centrosome and the bead differ in both plateau height and length in the double-logarithmic plot due to their different drag and optical properties, respectively. These two parameters are obtained from the fitting to the power spectral density equation described in Materials and Methods. As explained in that section, the former parameter is proportional to the drag coefficient of the trapped specimen, and the latter, which is not used here, is set by the so-called corner frequency.

Fig. 2, *A* and *B*, show the size distribution of the early *Drosophila* embryo centrosome measured by the two respective methods from individually manipulated specimens. A multiple-centrosome manipulation event can be detected because the size of the resulting aggregate approximately appears as a multiple of the distribution mean. Both methods yielded mean diameters for the centrosome that were remarkably larger than the EM mean diameter (0.75 μm (5,26); see also the Supporting Material), thus manifesting underlying hydrodynamic effects. The mean Stokes diameter is 1.21 $\pm$ 0.36 μm (~60% larger than the EM diameter), whereas that from the thermal-noise analysis is 0.95 $\pm$ 0.20 μm (~30% larger than the EM diameter). It is also interesting to note that the mean hydrodynamic diameters measured by the two methods differ. A linear regression for the size measured by both methods (correlation coefficient = 0.83) confirms that the Stokes diameter is 1.3 times greater than the thermal-noise-derived diameter. By contrast, no size differences were observed for the compact, solid particles used as reference (both methods agreed with the vendor's information; see the Supporting Material), which indicates that the centrosome's overall structure is flexible and diffusive in buffer solution. Specifically, although both methods deduce the diameter from the same physical magnitude (i.e., the drag coefficient), the range of distances over which the specimen is displaced is different and influences both the structure and size of the centrosome. In the Stokes law method, the whole centrosome is dragged over distances of micrometers (Fig. 1 *A*), whereas in the thermal-noise method, the centrosome describes smaller, nanometer-range position fluctuations in its hydrodynamic neighborhood (Fig. 1 *B*).

Given these results and the electronic measurements explained below, we will show that the EM diameter of the centrosome is smaller than its physiological size, because in the former case it is in dehydration conditions, and in the latter (in aqueous solution) it is subject to its own electric field. Because of the diffusive nature of the PCM, our results suggest that the hydrodynamic neighborhood of the centrosome

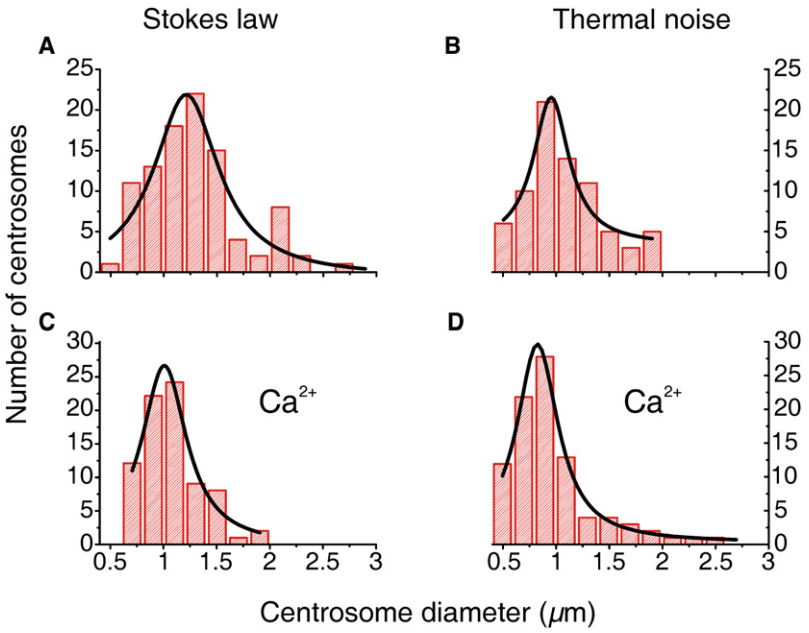

FIGURE 2 Hydrodynamic size of *Drosophila* centrosome in physiological conditions. Top row: Size distributions in BRB80 measured by (*A*) Stokes law ($n = 97$) and (*B*) thermal-noise analysis ($n = 75$). Bottom row: Size distributions in BRB80 with 5 mM $CaCl_2$ and no EGTA, measured by (*C*) Stokes law ($n = 78$) and (*D*) thermal-noise analysis ($n = 91$). Black lines in the histograms are Lorentzian fits. Size heterogeneity in the centrosome population may reflect either the progression of the nuclear cycles or the loss or gain of PCM throughout the centrosome purification procedure (26).

comprises not only water molecules and condensing counterions, which surround every charged structure in solution, but principally consists of proteinaceous fibrils belonging to the outer extent of the pericentriolar matrix (hereafter referred as the PCM neighborhood). The effective size measured by the thermal-noise method, therefore, is just that of a denser, thermally fluctuating core (hereafter referred as the centriole core), which should be constituted by the centrioles plus the proximal pericentriolar matrix (PCM neighborhood excluded).

Centrosome organization, as studied by EM, has been reported to vary in the presence of divalent cations (8,33). In particular, Ca^{2+} was shown to contract the bulk centrosome structure of the human lymphoblastoma KE37 cell line, a process that entails both the centriole structure and the PCM (33). To monitor this effect in physiological conditions, we used the same single-organelle approach, this time with *Drosophila* embryo centrosomes in BRB80 with 5 mM $CaCl_2$ and no EGTA. The resulting size distributions, shown in Fig. 2, *C* and *D*, are shifted toward shorter diameters, thus confirming a physiological contraction. The mean diameter is 1.00 ± 0.25 μm (20% reduction) as measured by Stokes law method, and 0.83 ± 0.24 μm (13% reduction) by the thermal-noise analysis, which indicates that Ca^{2+} has different effects on the two hydrodynamic centrosome domains; specifically, Ca^{2+} has a stronger influence on the centriole-core domain than on the PCM neighborhood. This is in agreement with a reported decrease in the intercentriolar distance in the presence of Ca^{2+} (33).

Electric behavior: the centrosome is a net negatively charged organelle with a very low isoelectric region

Optical tweezers are also capable of sensing ultrasmall, picoNewton forces, and thus provide a clearcut method for analyzing the electric properties of isolated specimens in different environments. With this method, analyses can be performed with low quantities of purified samples, which could limit other electrophoretic methods. Furthermore, the single-centrosome force signals caused by an electric field are not confused by either the simultaneous presence of other specimens or stochastic dynamics arising from crowding effects. As detailed in Materials and Methods, we assembled two 25-μm-thick electrode wires connected to a power supply inside the fluid chamber. The specimens were trapped halfway between the electrodes, as depicted in Fig. 3 *A*. We applied constant-voltage pulses of a few volts by switching the power supply on and off at intervals of ~1 s (i.e., a ~1-Hz rate) and average simultaneous recording of forces exerted on the individual specimens in the presence of the electric field over 17 ms (~60 Hz). The latter rate is below the corner frequency of the specimens in the optical trap, thus maintaining the low-frequency Brownian noise, and far above the stimulation rate, thus allowing time-resolved response detections. A 60-Hz measuring cutoff smoothes the force data sets by filtering out all the high-frequency background noise, such as high-frequency electronic noise. The circuit layout is such that a positive force implies a negatively charged specimen, which shifts toward the anode from its resting position in the optical trap (see Movie S2). Fig. 3 *B* (*left column*) shows single-centrosome individual assays in different buffers that cover a wide range of pH values (see Materials and Methods). As a control, streptavidin-coated, 2.10-μm-diameter polystyrene microspheres of known electrophoretic behavior were also assayed (Fig. 2 *B*, *right column*). Electric fields in solutions with significant ionic strength are subject to strong attenuation by counterionic screening, and therefore their strength decreases very quickly over a distance equal to several Debye lengths. We thus used

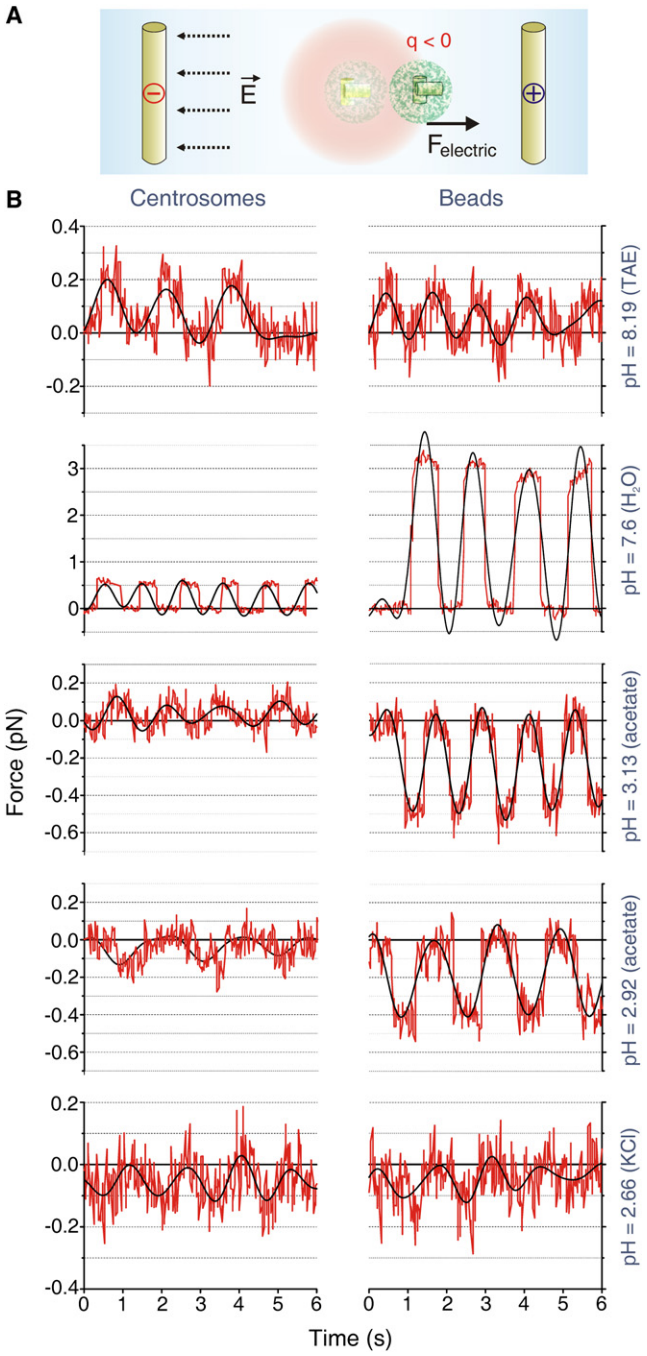

FIGURE 3 Electric force over single centrosomes at different pH values. (*A*) Experimental configuration: A single centrosome held in the optical trap is displaced from the center of the common lasers' focal spot (*red halo*; note that the light path is perpendicular to the plane of the plot) due to the electric field, *E*, between the two gold-plated tungsten electrodes (*yellow rods*). The circuit configuration is such that a positive force ($F_{electric}$) toward the anode implies a negatively charged specimen. (*B*) Centrosomes (*left column*) and streptavidin-coated, 2.10-μm-diameter beads (*right column*) were subjected to constant-voltage pulses of ~1 s. Note that force strengths depend not only on the pH, but also on both the ionic strength and mobility of the buffering salt species for a given applied voltage. We used pulses of 3.5 V, except in DI water (3.9 V and 4.3 V for the experiments with centrosomes and beads, respectively), and except for the experiments with beads in TAE (3.1 V). Black lines: Low-pass filtered data to 1 Hz.

low-ionic-strength buffers to increase the contrast of the electric response with respect to the background noise. In this respect, electric screening on both centrosomes and beads in BRB80 led to no observable force signal under our machine resolution (0.1 pN) (27); by contrast, the signal in DI water, with the lowest ionic strength, is clearly distinguished from the rapid background oscillations that arise from thermal and instrumental noise. Our results for streptavidin-coated beads show a force sign change in agreement with previously reported pI values for surface monolayers of streptavidin (i.e., pI = 5–5.5 (28); see the Supporting Material for an additional bulk mobility characterization of the sample beads). With regard to the centrosome, all of the individual specimens tested in buffers with pH $\geq$ 3.13 experienced a positive force (negative charge), whereas in those with pH $\leq$ 2.92, the force was always negative (positive charge). In the vicinity of pH 3.10, the charge was small and its sign differed from centrosome to centrosome. Therefore, these assays mark *Drosophila* centrosome isoelectricity in the region of pH 3.1 $\pm$ 0.1.

Estimations of the effective charge of the centrosome in addition to that at the shear plane of the streptavidin-coated beads used as reference (34) are shown in Table 1. As expected, near the pI, the centrosome approaches neutrality, thus showing its lowest net charge. Centrosome neutrality in the vicinity of pH $\approx$ 3.10 was also manifested by the gradual appearance of centrosome aggregates in the acetate buffer solution at this pH. In contrast, the net charge for streptavidin-coated polystyrene beads at this pH is much larger because the streptavidin molecules coating the beads are away from their pI (28). In DI water, both specimens exhibit very large charges because they are far from their respective pI and in conditions of both very low ionic strength and buffer conductivity. Near physiological conditions, the surface-charge density of the centrosome is smaller than that of microtubules, as discussed further below.

TABLE 1 Estimated effective charge of centrosomes and streptavidin-coated beads

		Net charge (e)*		Charge density† (C/m^2)	
Buffer	pH	centrosome	bead	centrosome	bead
KCl	2.66	$+9.4 \times 10^2$	$+1.4 \times 10^3$	$+4.4 \times 10^{-5}$	$+1.6 \times 10^{-5}$
Acetate	3.10	$+1.5 \times 10^2$	$+1.6 \times 10^3$	$+1.1 \times 10^{-5}$	$+1.9 \times 10^{-5}$
Acetate	3.13	-4.6×10^2	$+1.5 \times 10^3$	-3.6×10^{-5}	$+1.7 \times 10^{-5}$
DI H_2O	7.60	-5.0×10^3	-1.9×10^4	-2.7×10^{-4}	-2.2×10^{-4}
TAE	8.19	-2.1×10^3	-5.0×10^3	-9.3×10^{-5}	-5.8×10^{-5}

Geometrical features of both the fluid chamber and electrodes may affect the uniformity of the electric field. Retardation effects were not taken into account. To cover a wide range of pH, buffers were prepared from different chemical species, thus differing in ionic strengths and conductivities (see Materials and Methods). These facts affect the electric screening and consequently the charge magnitude of the bare specimen.

*e is the electron charge in absolute value (i.e., $+1.6021 \times 10^{-19}$ C).

†Estimated by taking into account the size versus pH behavior of the centrosome in Fig. 4.

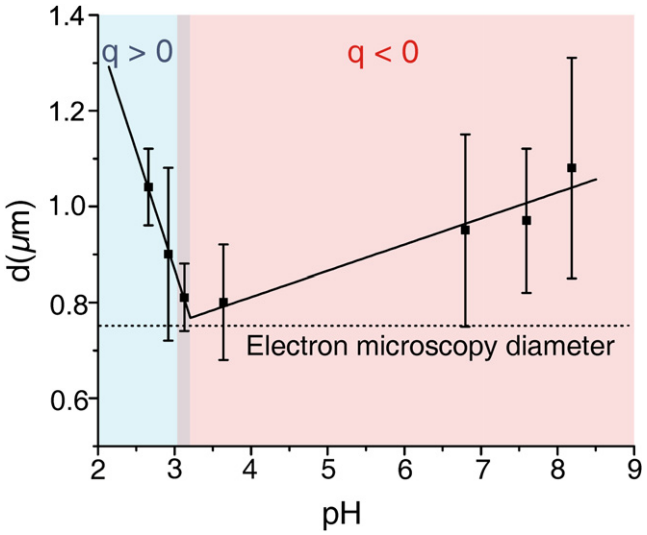

FIGURE 4 Effect of the pH on the centrosome size. Data points at each pH represent centrosome size distribution-mean values (measured by the thermal-noise method), and error bars are their corresponding full width at half-maximum. Note that different buffers have been used to cover the plotted range of pH (see Materials and Methods for details). The black lines are two independent linear regressions to the size data points corresponding to the two different electric behaviors of the centrosome with pH ($q > 0$ and $q < 0$). The red background indicates a negative-charge pH region ($q < 0$), and the blue background indicates a positive-charge pH region ($q > 0$). The vertical shaded bar delimits the isoelectric region. The horizontal dashed line marks the *Drosophila* centrosome size determined by EM (26).

The electric field of the centrosome self-induces a pH-dependent structural dynamics

Before each electric assay, we obtained a size measurement of each sample centrosome by thermal-noise analysis. As shown in Fig. 4, a plot of size versus pH reveals that the centrosome dimensions decrease monotonously from both high and low pH to attain a minimum size near the pH where the specimen shows isoelectricity. By modeling both size decays with the simplest trend, that is, linear with pH, we obtain a minimum mean diameter of 0.77 ± 0.15 μm at the crossing point. This value for the neutral specimen is very similar to the above-mentioned mean diameter measured for dehydrated EM samples: 0.75 μm (4,26). The correspondence between both values is expected, since both experimental conditions produce no electric influence on the centrosome. The large size variations observed with pH for the centrosome, together with those previously discussed in the presence of Ca^{2+}, cannot be generated solely by organization events of both water molecules and condensing counterions around its structure, because, as in the analysis of Ca^{2+} effects, no such size variations were appreciated for the streptavidin-coated beads used as reference in different buffers and pH (data not shown). Therefore, we suggest that the electric field of the centrosome, which proves to be regulated by pH, produces an electrophysiological, self-structural dynamics that involves both the PCM neighborhood and the centriole core. The isolation conditions and subsequent manipulation steps of the centrosome do not allow microtubule nucleation; however, any incipient, short microtubules that might have nucleated in the sample centrosomes cannot explain this structural behavior because their persistence length is too large compared to the centrosome size (35).

Variations in intracellular pH with both time (cell cycle) and position are known to occur in vivo (36). However, given the larger pH changes used in this work, we studied the reversibility of our results with the aim of detecting any overall damage to the organelle in acidic conditions. To that end, centrosomes were flowed from acetate buffer with pH 2.92, where, as shown in Fig. 4, the charge was positive and the size was 0.90 ± 0.18 μm, into a fluid chamber filled with TAE at pH 8.19, where the charge was negative and the size was 1.08 ± 0.23 μm. We found that the negative charge behavior recovered, and that during the few seconds required for the experiment, the size increased, according to the trend in Fig. 4, up to a value of 0.95 ± 0.23 μm. A similar size change, this time a reduction from 1.08 ± 0.23 to 0.99 ± 0.05 μm, was observed when centrosomes were flowed from a TAE buffer into a fluid chamber filled with acetate buffer. The recovery of both the charge sign and the size trend with pH in these tests suggests that low pH conditions produce neither a strong, irreversible denaturation of the centrosome core structure nor a large PCM loss.

DISCUSSION

The centrosome is a central organelle in animal cells and is involved in elementary cellular processes such as microtubule organization, which is fundamental for cell motility and adhesion, and cell division. Electric phenomena, which are key to understanding molecular structure and interactions, have important implications in cellular processes because every cellular component carries an associated electric behavior.

With regard to the cytoplasm, the centrosome net negative charge measured here under in vitro conditions, as well as the influence of endogenous electric fields, such as those originating from membranes and microtubules (9,12,13,32), will have major implications in vivo on the nanoscale (distances on the order of the Debye length), and may produce background effects on larger distances (14,15,17,37) at timescales longer than the millisecond. When we compare our measurements with the results of previous electrophoresis experiments on microtubules (12,13), we observe that the centrosome's effective surface-charge density in physiological pH has the same sign but is significantly smaller, in absolute value, than that of microtubules, according to an effective surface-charge density of $(-3.67 \pm 0.04) \times 10^{-2}$ C/m^2 for microtubules (pH 6.9) (13) and our data in Table 1 for the early *Drosophila* embryo centrosome. Besides the pH-dependent self-modulating structural effect reported here, the electric

field draining to the negatively charged centrosome in vivo may be sufficient to drive tubulin dimers in the vicinity of the centrosome into parallel alignment with respect to the electric near-field lines by providing torque equilibrium to the tubulin dipole (12,32). This inherent effect can combine with the action of recently reported microtubule polymerases (24,25) on tubulin dimers that diffuse in the vicinity of the centrosome. It is also noteworthy that the α-β arrangement of the tubulin dimer relative to the centrosome is consistent with the stability that electric forces would give to the early growing microtubule in the absence of other phenomena, according to the charge distribution of the microtubule ends (38). In addition, a net negative charge on both the centrosome and the microtubules may help explain why the latter initially grow with radial directionality from the centrosome. Concurrently, the corresponding lateral negative charge of microtubules at physiological pH that nucleate off the centrosome may contribute to this effect by generating repelling forces amid the nascent microtubules up to separation distances where their charges are electrically screened. As a consequence, near-field electric forces could have an important role in the early organization of aster microtubule bundles. The larger lateral electric fields stemming from microtubules may later be required to assemble the mitotic spindle by preventing microtubule heaping, thus enabling fine arranging mechanisms, regulated by both pH and ions (39), and microtubule-associated proteins (40), as well as a molecular-motor-mediated fine control of the sliding mechanisms (41).

CONCLUSIONS

We have revealed the electric charge of the centrosome and its structural implications. Because of the structural contrast between the diffusive PCM and the more compact core of centrioles, we were able to obtain measurements of the drag coefficient by means of the Stokes law and thermal-fluctuation spectral analysis of force, which differ in the range of distances over which the specimen is displaced, to discriminate two dynamic centrosome domains by their thermally induced fluctuations. These dynamic domains are the outermost PCM fibril matrix (PCM neighborhood) and the more condensed internal part comprised of the core of centrioles plus the innermost PCM (centriole core). These dynamic distinction and biophysical properties were determined by laser-based manipulation of individual centrosomes in physiological conditions, which, from a methodological viewpoint, afforded single-organelle electrophoresis. This approach is specific, irrespective of the molecular composition and structural organization of the specimen, and it provides univocal signals from individual specimens that are not confused by crowding effects. This method can also be used to study the sensitivity of centrosomes to different environmental conditions, and to follow the progression of the centrosome cycle.

We believe that this methodology opens the way to electric and hydrodynamic characterizations of other organelles and large supramolecular assemblies. For the latter, although the measured drag coefficient in a dynamic situation would be of representative, physiological interest, fluctuations and trapping orientations would require a more in-depth consideration of size measurements in nonspherical organelles to ensure a certain degree of accuracy. The electric and hydrodynamic behaviors of a centrosome caused by cell-cycle variations of pH may further produce direct effects on mitosis.

SUPPORTING MATERIAL

Materials and methods, a table, a figure and two movies are available at http://www.biophysj.org/biophysj/supplemental/S0006-3495(09)01055-8.

We thank C. Bustamante and S.B. Smith for help in setting up the optical-tweezers laboratory, C. González and J. Reina for valuable discussions, P. Tartaj for electrophoretic mobility characterization of polystyrene beads, and M. Serna and M.J. Rodríguez for biochemical and EM support, respectively.

This work was supported by grants from the Spanish Ministry of Science and Innovation (BFU2005-06487, CSD2006-00023, BFU2007-62382/BMC, and BFU2008-02328/BMC) and the Comunidad de Madrid (S-0505/MAT/0283). S.H. received a scholarship from Consejería de Educación de la Comunidad de Madrid and the European Social Fund. J.R.A.-G. was the recipient of an individual fellowship from the International Human Frontier Science Program Organization and a Ramón y Cajal contract from the Spanish Ministry of Science and Innovation.

REFERENCES

1. Doxsey, S. 2001. Re-evaluating centrosome function. *Nat. Rev. Mol. Cell Biol.* 2:688–698.
2. Bettencourt-Dias, M., and D. M. Glover. 2007. Centrosome biogenesis and function: centrosomics brings new understanding. *Nat. Rev. Mol. Cell Biol.* 460:451–463.
3. Bornens, M. 2002. Centrosome composition and microtubule anchoring mechanisms. *Curr. Opin. Cell Biol.* 14:25–34.
4. Lange, B. M. H., and K. Gull. 1996. Structure and function of the centriole in animal cells: progress and questions. *Trends Cell Biol.* 6:348–352.
5. Moritz, M., M. B. Braunfeld, J. C. Fung, J. W. Sedat, B. M. Alberts, et al. 1995. Three-dimensional structural characterization of centrosomes from early *Drosophila* embryos. *J. Cell Biol.* 130:1149–1159.
6. Ibrahim, R., C. Messaoudi, F. J. Chichon, C. Celati, and S. Marco. 2009. Electron tomography study of isolated human centrioles. *Microsc. Res. Tech.* 72:42–48.
7. Gonzalez, C., G. Tavosanis, and C. Mollinari. 1998. Centrosomes and microtubule organization during *Drosophila* development. *J. Cell Sci.* 111:2697–2706.
8. Baron, A. T., V. J. Suman, E. Nemeth, and J. L. Salisbury. 1994. The pericentriolar lattice of PTK2 cells exhibits temperature and calcium-modulated behavior. *J. Cell Sci.* 107:2993–3003.
9. McCaig, C. D., A. M. Rajnicek, B. Song, and M. Zhao. 2005. Controlling cell behavior electrically: Current views and future potential. *Physiol. Rev.* 85:943–978.
10. Tyner, K. M., R. Kopelman, and M. A. Philbert. 2007. "Nanosized voltmeter" enables cellular-wide electric field mapping. *Biophys. J.* 93:1163–1174.
11. Kovacic, P. 2008. Bioelectrostatics: review of widespread importance in biochemistry. *J. Electrostat.* 66:124–129.

12. Stracke, R., K. J. Böhm, L. Wollweber, J. A. Tuszynski, and E. Unger. 2002. Analysis of the migration behavior of single microtubules in electric fields. *Biochem. Biophys. Res. Commun.* 293:602–609.

13. van den Heuvel, M. G. L., M. P. de Graaff, S. G. Lemay, and C. Dekker. 2007. Electrophoresis of individual microtubules in microchannels. *Proc. Natl. Acad. Sci. USA.* 104:7770–7775.

14. Gagliardi, L. J. 2002. Electrostatic force in prometaphase, metaphase, and anaphase-A chromosome motions. *Phys. Rev. E.* 66:011901.

15. Gagliardi, L. J. 2008. Induced electrostatic charge in poleward motion of chromosomes during mitosis. *J. Electrostat.* 66:147–155.

16. Vassilev, P. H., and M. Kanazirska. 1985. The role of cytoskeleton in the mechanisms of electric field effects and information transfer in cellular systems. *Med. Hypotheses.* 16:93–96.

17. Zhao, M., J. V. Forrester, and C. D. McCaig. 1999. A small, physiological electric field orients cell division. *Proc. Natl. Acad. Sci. USA.* 96:4942–4946.

18. Detrich, III, H. W., and S. A. Overton. 1986. Heterogeneity and structure of brain tubulins from cold-adapted Antarctic fishes. Comparison to brain tubulins from a temperate fish and a mammal. *J. Biol. Chem.* 261:10922–10930.

19. Linhartová, I., E. Dráberová, V. Viklický, and P. Dráber. 1993. Distribution of non-class-III β-tubulin isoforms in neuronal and non-neuronal cells. *FEBS Lett.* 320:79–82.

20. Hormeño, S., and J. R. Arias-Gonzalez. 2006. Exploring mechanochemical processes in the cell with optical tweezers. *Biol. Cell.* 98:679–695.

21. Ashkin, A., and J. M. Dziedzic. 1987. Optical trapping and manipulation of viruses and bacteria. *Science.* 235:1517–1520.

22. Ashkin, A., and J. M. Dziedzic. 1989. Internal cell manipulation using infrared laser traps. *Proc. Natl. Acad. Sci. USA.* 86:7914–7918.

23. Fuhr, G., Th. Schnelle, T. Müller, H. Hitzler, S. Monajembashi, et al. 1998. Force measurements of optical tweezers in electro-optical cages. *Appl. Phys. A.* 67:385–390.

24. Brouhard, G. J., J. H. Stear, T. L. Noetzel, J. Al-Bassam, K. Kinoshita, et al. 2008. XMAP215 is a processive microtubule polymerase. *Cell.* 132:79–88.

25. Barr, A. R., and F. Gergely. 2008. MCAK-independent functions of ch-Tog/XMAP215 in microtubule plus-end dynamics. *Mol. Cell. Biol.* 28:7199–7211.

26. Lange, B. M. H., G. Kirfel, I. Gestmann, V. Herzog, and C. Gonzalez. 2005. Structure and microtubule-nucleation activity of isolated *Drosophila* embryo centrosomes characterized by whole mount scanning and transmission electron microscopy. *Histochem. Cell Biol.* 124:325–334.

27. Smith, S. B., Y. Cui, and C. Bustamante. 2003. An optical-trap force transducer that operates by direct measurement of light momentum. *Methods Enzymol.* 361:134–162.

28. Sivasankar, S., S. Subramaniam, and D. Leckband. 1998. Direct molecular level measurements of the electrostatic properties of a protein surface. *Proc. Natl. Acad. Sci. USA.* 95:12961–12966.

29. Wang, M. C., and G. E. Uhlenbeck. 1945. On the theory of the Brownian motion II. *Rev. Mod. Phys.* 17:323–342.

30. Berg-Sørensen, K., and H. Flyvbjerg. 2004. Power spectrum analysis for optical tweezers. *Rev. Sci. Instrum.* 75:594–612.

31. Mao, H., J. R. Arias-Gonzalez, S. B. Smith, I. Tinoco, and C. Bustamante. 2005. Temperature control methods in a laser tweezers system. *Biophys. J.* 89:1308–1316.

32. Mershin, A., A. A. Kolomenski, H. A. Schuessler, and D. V. Nanopoulos. 2004. Tubulin dipole moment, dielectric constant and quantum behavior: computer simulations, experimental results and suggestions. *Biosystems.* 77:73–85.

33. Paintrand, M., M. Moudjou, H. Delacroix, and M. Bornens. 1992. Centrosome organization and centriole architecture: their sensitivity to divalent cations. *J. Struct. Biol.* 108:107–128.

34. Wada, K., K. Sasaki, and H. Masuhara. 2002. Electric charge measurement on a single microparticle using thermodynamic analysis of electrostatic forces. *Appl. Phys. Lett.* 81:1768–1770.

35. van den Heuvel, M. G. L., M. P. de Graaff, and C. Dekker. 2008. Microtubule curvatures under perpendicular electric forces reveal a low persistente length. *Proc. Natl. Acad. Sci. USA.* 105:7941–7946.

36. Madshus, I. H. 1988. Regulation of intracellular pH in eukaryotic cells. *Biochem. J.* 250:1–8.

37. Pokorný, J., F. Jelínek, and V. Trkal. 1998. Electric field around microtubules. *Bioelectrochem. Bioenerg.* 45:239–245.

38. Baker, N. A., D. Sept, S. Joseph, M. J. Holst, and A. McCammon. 2001. Electrostatics of nanosystems: Application to microtubules and the ribosome. *Proc. Natl. Acad. Sci. USA.* 98:10037–10041.

39. Stebbings, H., and C. Hunt. 1982. The nature of the clear zone around microtubules. *Cell Tissue Res.* 227:609–617.

40. Hirokawa, N. 1994. Microtubule organization and dynamics dependent on microtubule-associated proteins. *Curr. Opin. Cell Biol.* 6:74–81.

41. Sharp, D. J., G. C. Rogers, and M. J. Scholey. 2000. Microtubule motors in mitosis. *Nature.* 407:41–47.